Enzyme and Microbial Technology 69 (2015) 1–9

Contents lists available at ScienceDirect

Enzyme and Microbial Technology

journal homepage: www.elsevier.com/locate/emt

Characterization of glutathione *S*-transferases from *Sus scrofa*, *Cydia pomonella* and *Triticum aestivum*: Their responses to cantharidin

Xue-Qing Yang [a,b], Ya-Lin Zhang [a,*]

[a] *Key Laboratory of Plant Protection Resources & Pest Management of the Ministry of Education, College of Plant Protection, Northwest A & F University, Yangling, Shaanxi 712100, China*
[b] *College of Plant Protection, Shenyang Agricultural University, Shenyang 110866, Liaoning, China*

ARTICLE INFO

Article history:
Received 15 September 2014
Received in revised form 6 November 2014
Accepted 14 November 2014
Available online 24 November 2014

Keywords:
Glutathione *S*-transferases
Cantharidin
Stress
Biochemical characterization
Binding protein

ABSTRACT

Glutathione *S*-transferases (GSTs) play a key role in detoxification of xenobiotics in organisms. However, their other functions, especially response to the natural toxin cantharidin produced by beetles in the Meloidae and Oedemeridae families, are less known. We obtained GST cDNAs from three sources: *Cydia pomonella* (*CpGSTd1*), *Sus scrofa* (*SsGSTα1*), and *Triticum aestivum* (*TaGSTf3*). The predicted molecular mass is 24.19, 25.28 and 24.49 kDa, respectively. These proteins contain typical N-terminal and C-terminal domains. Recombinant GSTs were heterologously expressed in *Escherichia coli* as soluble fusion proteins. Their optimal activities are exhibited at pH 7.0–7.5 at 30 °C. Activity of CpGSTd1 is strongly inhibited by cantharidin and cantharidic acid, but is only slightly suppressed by the demethylated analog of cantharidin and cantharidic acid. Enzymatic assays revealed that cantharidin has no effect on SsGSTα1 activity, while it significantly stimulates TaGSTf3 activity, with an EC_{50} value of 0.3852 mM. Activities of these proteins are potently inhibited by the known GST competitive inhibitor: *S*-hexylglutathione (GTX). Our results suggest that these GSTs from different sources share similar structural and biochemical characteristics. Our results also suggest that CpGSTd1 might act as a binding protein with cantharidin and its analogs.

1. Introduction

Mammals, insects, and plants are continuously exposed to xenobiotics, compounds that may cause toxic and sometimes lethal effects [1]. The naturally occurring toxicant cantharidin, the active ingredient of cantharides, is predominantly produced by *Cantharis vesicatoria* [2]. Cantharidin was recently reported to possess insecticidal toxicity [2–4] and its emulsifiable concentrate (EC) formulation has been developed into a bio-pesticide. Apart from its insecticidal activity, endothall, one of the cantharidin analogs, has been developed into a commercial herbicide that inhibits the protein phosphatase 2A (PP2A) activity in plants [5,6]. Cantharidin and its analog residues may interact deleteriously with mammals during feeding. To survive the effects of these naturally occurring xenobiotic compounds, organisms have evolved intricate biological adaptation mechanisms [7].

Glutathione *S*-transferases (GSTs, EC 2.5.1.18) are dimeric proteins existing in both prokaryotic and eukaryotic organisms involved in cellular detoxification. They catalyze the conjugation of glutathione (GSH) with a wide range of endogenous and exogenous agents, including carcinogens, therapeutic drugs, pesticides, environmental toxins and products of oxidative stress [8–10]. GSTs are also responsible for regulating important cell signaling pathways and biosynthesis [10]. To date, there are three categories of GSTs: cytosolic, microsomal and mitochondrial [10,11]. Mammal cytosolic GSTs are further divided into seven classes: alpha, mu, pi, sigma, omega, zeta and theta [10]. The class alpha contains many possible isoenzymes with different activities, tissue distribution and substrate specificities. Insect cytosolic GSTs are divided into six classes: delta, epsilon, omega, sigma, theta, and zeta [12]. The delta and epsilon classes are arthropod-specific GSTs involved in the detoxification of xenobiotics [9,13]. Plant cytosolic GSTs are grouped into seven classes: theta, zeta, phi, tau, lambda, glutathione-dependant dehydroascorbate reductase (DHAR), and tetrachlorohydroquinone dehalogenase [14]. The phi and tau GST subfamilies are responsible for herbicide detoxification [15].

Many GSTs have been isolated and characterized from bacteria, plants, insects, fish and mammals [8]. Recent studies suggest that cantharidin possesses insecticidal toxicity and inhibits the activity of insect GSTs [2–4]. However, knowledge about the

* Corresponding author. Tel.: +86 29 87092190; fax: +86 29 87092190.
E-mail address: yalinzh@nwsuaf.edu.cn (Y.-L. Zhang).

http://dx.doi.org/10.1016/j.enzmictec.2014.11.003
0141-0229/

Table 1
PCR primers used in this study.

Name	Sequence (5′–3′)	Primer used
SsGSTα1F	C***GGATCC*** ATGGCGGGGAAGCCCATTC	Cloning SsGSTα1 ORF
SsGSTα1R	T***AAGCTT***TTAATCCGGAAAATATTCTTG	
CpGSTd1F	C***GGATCC***ATGCCAGACCTATACTACG	Cloning CpGSTd1 ORF
CpGSTd1R	T***AAGCTT***TTACTTCTTCATCATGCTG	
TaGSTf3F	C***GGATCC***ATGGCGCCGGCGGTGAAGG	Cloning TaGSTf3 ORF
TaGSTf3R	T***AAGCTT***CTACTCTGCTTTCTTTCCAAG	

The start codon and stop codon are underlined. The *Bam*H I and *Hin*d III restriction enzyme sites are in italicized bold.

effect of cantharidin on GSTs from other organisms, especially mammals and plants is poorly known. In this study, we identified different classes of GST from three sources, including alpha class GST *Sus scrofa* (SsGSTα1, GenBank accession no. NM_214389.1), delta class GST from *Cydia pomonella* (CpGSTd1, GenBank accession no. EU887533.1), and phi class GST from *Triticum aestivum* (TaGSTf3, GenBank accession no. AJ440792.1), representing mammals, insects, and plants, respectively. The recombinant biochemical properties, sensitivity to inhibitors and response to cantharidin and its analogs of recombinant GST proteins were investigated.

2. Experiment

2.1. Materials

Escherichia coli strains DH5α and BL21 (DE3) were used as host cells and were cultivated according to the instructions of the suppliers (Takara, Dalian, China). The restriction enzyme and *Taq* polymerase were also obtained from Takara (Takara). Cantharidin and norcantharidin were obtained from Alfa Aesar Chemical Co. Ltd. (Haverhill, MA, USA). Their analogs, cantharidic acid and norcantharidic acid (purity > 95%) were previously synthesized [16]. The GST inhibitor [17] *S*-hexylglutathione (GTX) was purchased from Aladdin Reagent (Shanghai, China). The 1-chloro-2,4-dinitrobenzene (CDNB) and reduced glutathione were purchased from ABCR GmbH & CO. KG (Germany) and Sigma–Aldrich Life Sciences (St. Louis, MO), respectively. Other chemicals and reagents were commercially available. The cDNAs from *S. scrofa* liver and *T. aestivum* lamina were kindly supplied by the College of Animal Science and Technology, and the State Key Laboratory of Crop Stress Biology for Arid Areas (Northwest A & F University, China), respectively.

2.2. Sequence analysis of GSTs

The amino acid sequences of *SsGSTα1*, *CpGSTd1* and *TaGSTf3* were deduced and the theoretical isoelectric point (*pI*) of the deduced proteins were predicted using ExPASy Proteomics [18]. The amino acid sequence of SsGSTα1, CpGSTd1 and TaGSTf3 were aligned using Clustal W2 (http://www.ebi.ac.uk/Tools/msa/clustalw2). A similarity analysis of SsGSTα1, CpGSTd1 and TaGSTf3 was performed using the BLAST web program (http://blast.ncbi.nlm.nih.gov/Blast.cgi). The secondary structure of these proteins was predicted using PSIPRED [19]. Phylogenetic analyses were constructed by using MEGA4 [20] using the neighbor-joining method with 1000 bootstrap replicates.

2.3. GSTs isolation and construction of the expression plasmid

The total RNA of *C. pomonella* was extracted from five third instar larvae using the RNAiso Plus Kit (Takara) according to the manufacturer's instructions. The RNA was then digested with DNase I (MBI, Fermentas) to remove the genomic DNA. Subsequently, the first strand cDNA was synthesized from 1 μg of total RNA using the RevertAid™ First Strand cDNA synthesis kit (MBI) as described by the manufacturer. The ORF of *SsGSTα1*, *CpGSTd1* and *TaGSTf3* were amplified using the following primer pairs: SsGSTα1F and SsGSTα1R, CpGSTd1F and CpGSTd1R, and TaGSTf3F and TaGSTf3R, respectively. These primers were introduced into *Bam*H I and *Hin*d III restriction enzyme sites as the forward and reverse primer (Table 1), respectively. PCR was performed on a C1000 Thermal Cycler (BioRad, USA) using high-fidelity Ex *Taq* polymerase (Takara) to eliminate any potential error occurring with *Taq* DNA polymerase. The PCR product was gel purified using the Biospin Gel Extraction Kit (Bioer Technology Co., Ltd, China) and cloned into pMD-19T vector (Takara), and then transferred into *E. coli* DH5α (Takara). The sequenced plasmid (Shanghai Sunny Biotech Co., Ltd, China) was digested by *Bam*H I and *Hin*d III, and thereafter cloned into the expression vector pET-32a (+) and transformed into the host strain, *E. coli* BL21(DE3).

2.4. Expression and purification of recombinant GSTs

The positive *E. coli* colonies were grown in 400 ml of Luria-Bertani (LB) medium containing 100 μg ml^{-1} ampicillin. After OD_{600} reached 0.6, the recombinant GST expression was induced with a 0.2 mM final concentration of isopropyl β-D-thiogalactopyranoside (IPTG) at 25 °C with shaking at 220 rpm for 12 h.

Bacterial cells were harvested by centrifugation at 8000 × *g* for 10 min. The pellets were re-suspended in lysis buffer (10 mM Tris–HCl, 1 mg ml^{-1} lysozyme, pH 8.0) and incubated at room temperature for 30 min. After sonication for 5 min on ice, the supernatant was separated by centrifugation at 12,000 × *g* for 30 min at 4 °C. The soluble fraction was loaded onto a Ni^{2+}-NTA agarose gel column (TRANS, China) and recombinant protein was purified [21]. Eluted fractions were analyzed on a 12% SDS-PAGE gel (BioRad, USA). The target protein was dialyzed against sodium phosphate buffer (50 mM, pH 7.2) overnight to desalt. The concentration of purified protein was quantified by the Bradford method [22].

2.5. Enzyme kinetic properties of purified GSTs

The kinetic constants of purified recombinant GSTs were determined using 0.01–1.6 mM of CDNB (with GSH held constant at 10 mM), or 0.0625–4 mM of GSH (with CDNB held constant at 2 mM) in 50 mM sodium phosphate buffer (pH 7.2) at 30 °C. GST activity was measured as described previously [11]. The difference in absorbance value at time 1 min (t_1) and at time zero (t_0) was used to calculate activity. Results were expressed as nM glutathione conjugated mg of protein^{-1} min^{-1} (ε = 9.6 mM^{-1} cm^{-1}). The protein replaced by sodium phosphate buffer was used as the control. Each test was conducted in triplicate. The rate of reaction was used to construct a double-reciprocal Lineweaver–Burk plot of 1/*V versus* 1/*S*, and the kinetic constants, Michaelis constants (K_m) and V_{max} were determined.

2.6. Effect of pH and temperature on GSTs activities

Effects of pH on the activities of SsGSTα1, CpGSTd1 and TaGSTf3 were determined by using a varying pH (4.0–9.0) with sodium phosphate buffer (50 mM). The effects of temperature on the activities of SsGSTα1, CpGSTd1 and TaGSTf3 were measured by performing the reaction at temperatures ranging from 15 to 45 °C.

2.7. Effects of cantharidin and its analogs on GSTs activities

To investigate the effects of cantharidin and its analogs on GSTs activities, the purified CpGSTd1 was pre-incubated under final concentrations of 4 mM cantharidin, norcantharidin, cantharidic acid and norcantharidic acid, respectively, for 5 min at 30 °C before the addition of CDNB. Remaining activity was measured and CpGSTd1 replaced by sodium phosphate buffer was used as the control.

The effects under different concentrations of cantharidin on SsGSTα1, CpGSTd1 and TaGSTf3 activity were determined by pre-incubating 2 μl protein with 2, 0.2, and 0.02 mM cantharidin for 5 min. The reaction then was initiated by adding CDNB. The remaining activity was measured. For the positive control, the GTX was used and its half-inhibitory concentrations (IC_{50}) on SsGSTα1, CpGSTd1 and TaGSTf3 were determined.

2.8. Structural modeling for GSTs

3D structure of SsGSTα1 and TaGSTf3 were predicted using homology modeling (automated mode) using the SWISS-MODEL (http://swissmodel.expasy.org). The target template sequence was searched using BLAST against the primary amino acid sequence contained in the SWISS-MODEL template library. A total of 157 templates were found. For each identified template, the template's quality was predicted from features of the target-template alignment. The templates with the highest quality were then selected for model building. Thus, a 1.80 Å resolution crystal structure of Glutathione *S*-transferase A3 from the human (PDB no. 2vcv.1.A) and a 2.80 Å resolution crystal structure of *Arabidopsis thaliana* (araGST) (PDB no. 1bye.1.B) were selected from the PDB database and used as the templates for SsGSTα1 and TaGSTf3, respectively.

2.9. Statistical analysis

Statistical analysis was conducted using SPSS 12.0 (IBM, Chicago, USA). The effects of cantharidin and its analogs on GSTs activities were statistically analyzed using Student's *t*-test ($^*P \le 0.05$; $^{**}P \le 0.01$; $^{***}P \le 0.001$). Results are shown as the mean of triplicates ± standard deviation (SD) and were plotted using GraphPad Prism 5 (San Diego, USA).

3. Results

3.1. Molecular and sequence analysis of GSTs

The open reading frame of *CpGSTd1*, *SsGSTα1* and *TaGSTf3* were 648, 669 and 669 bp, respectively, encoding CpGSTd1, SsGSTα1 and

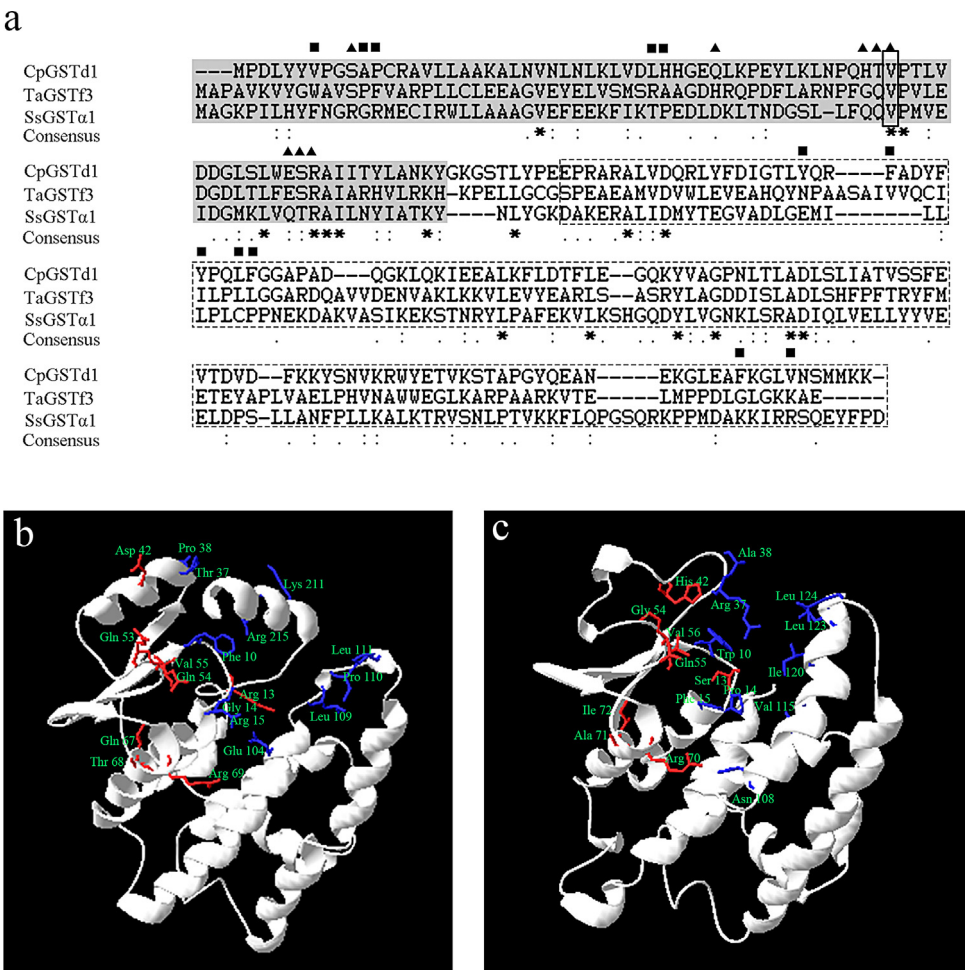

Fig. 1. Sequence alignment of CpGSTd1, TaGSTf3 and SsGSTα1. (a) The N-terminal domain is in gray. The C-terminal domain is the dash line boxed. The Val 53 is boxed. The symbols at the top of the alignment indicate those residues in CpGSTd1 that form the G-site (▲) and the H-site (■). Asterisks (*) indicate identical residues among three sequences; colons (:) indicate residues with conserved substitutions; dots (.) represent residues that are weakly conserved among three sequences. 3D structure of SsGSTα1 (b) and TaGSTf3 (c). The Arg 13, Asp 42, Gln 53, Gln 54, Val 55, Gln 67, Thr 68 and Arg 69 in SsGSTα1, and the Ser 13, His 42, Gly 54, Gln 55, Val 56, Arg 70, Ala 71 and Ile 72 in TaGSTf3 that form the G-site are shown in red. The Phe 10, Gly 14, Arg 15, Thr 37, Pro 38, Glu 104, Leu 109, Pro110, Leu111, Lys 211, and Arg 215 in SsGSTα1, and the Trp 10, Pro 14, Phe 15, Arg 37, Ala 38, Asn 108, Val 115, Ile 120, Leu 123 and Leu 124 in TaGSTf3 that form the H-site are shown in blue. (For interpretation of the references to color in this figure legend, the reader is referred to the web version of this article.)

TaGSTf3 proteins of 215, 222 and 222 amino acids, respectively. The CpGSTd1, SsGSTα1 and TaGSTf3 proteins had a predicted molecular mass of 24.19, 25.28 and 24.49 kDa, respectively. The CpGSTd1, SsGSTα1 and TaGSTf3 had a theoretical isoelectric point of 6.84, 8.86 and 5.30, respectively. The PSIPRED program prediction indicated that both the SsGSTα1 and TaGSTf3 contain two domains, an N-terminal domain and a C-terminal domain (Fig. 1a). The N-terminal domain of SsGSTα1 is composed of residues 1–79, and the C-terminal domain consists of residues 85–222. For TaGSTf3, its N-terminal domain of SsGSTα1 is composed of residues 1–80, and the C-terminal domain consists of residues 89–222. The catalytic-related serine residue is absent in SsGSTα1 (Fig. 1a).

The BLAST comparison indicates that SsGSTα1 displays more than an 80% amino acid identity with known mammal GSTs, and the TaGSTf3 exhibited more than 50% amino acid homology with known Gramineae plant GSTs. Moreover, the SsGSTα1 shares only 12.15% and 13.95% sequence identity with TaGSTf3 and CpGSTd1, and the TaGSTf3 shares an 18.14% amino acid homology with CpGSTd1 (Fig. 1a). However, their second structure, especially the G-site, is relatively conserved, suggesting that the CpGSTd1, SsGSTα1 and TaGSTf3 might have a similar function in the cellular detoxification of xenobiotics, including cantharidin (Fig. 1a).

3.2. Phylogenetic characterization of GSTs

To determine the evolutionary relationship of CpGSTd1, SsGSTα1 and TaGSTf3, we constructed an un-rooted phylogenetic tree using the neighbor-joining method with a bootstrap test with 1000 replicates. 60 GSTs, including 17 from Gramineae plant GSTs, 16 from mammal GSTs, and 27 from insect GSTs were derived from GenBank and analyzed (Fig. 2). The selected GSTs from mammals, Gramineae plants and insects form an independent cluster. The GST clusters from insects and mammals are derived from the same branch which parallels evolution with the branch composed of Gramineae plant GSTs, suggesting that these plants GSTs have a longer evolutionary history and higher genetic diversity than the GST from insects and mammals. The phylogenetic analysis also shows that the mammal GSTs appear to share a common ancestor with insect GSTs.

3.3. Illustration of GSTs structural model

The 3D structure of SsGSTα1 (Fig. 1b) and TaGSTf3 (Fig. 1c) were constructed using the X-ray structure of human Glutathione *S*-transferase A3 (PDB no. 2vcv.1.A, resolution 1.80 Å) and *A. thaliana*

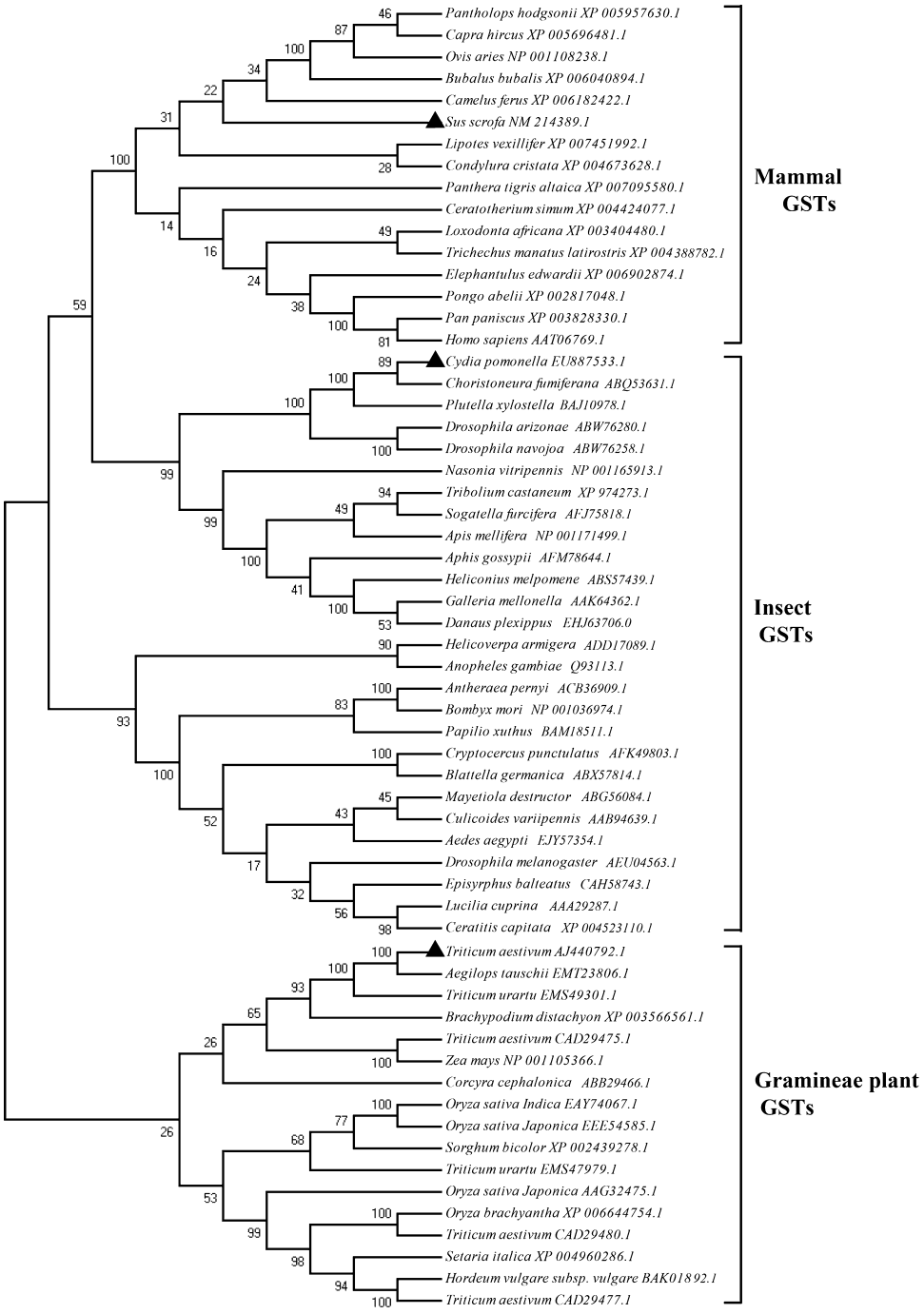

Fig. 2. An un-rooted neighbor-joining tree showing the phylogenetic relationship of GST from mammals, insects and Gramineae plants. Nodes indicate bootstrap calculated with 1000 replications support. The CpGSTd1, SsGSTα1 and TaGSTf3 are shown using "▲".

GST (araGST) (PDB no. 1bye.1.B, resolution 2.80 Å) as templates, respectively. The 3D structure of CpGSTd1 has been reported in a previous study [11] using the structure of *Anopheles gambiae* AgGSTd1-6 (PDB: 1PN9_B) as the template. The SsGSTα1, CpGSTd1 and TaGSTf3 shared 54%, 60% and 45% sequence identity with its corresponding template. Similar to homologous cytosolic GSTs, the SsGSTα1, CpGSTd1 and TaGSTf3 all comprised an N-terminal and a C-terminal domain (Fig. 1a), with an active site located in a cleft between the two domains which contains the glutathione binding site (G-site) and the hydrophobic binding site (H-site).

3.4. Expression and purification of recombinant proteins

To characterize the biochemical properties of the recombinant CpGSTd1, SsGSTα1 and TaGSTf3 *in vitro*, the ORFs of *CpGSTd1*, *SsGSTα1* and *TaGSTf3* were inserted into the pET-32a (+) vector. The recombinant N-terminal Trx, His, S-tagged CpGSTd1, SsGSTα1 and TaGSTf3 proteins were overexpressed in *E. coli* Bl21 (DE3) and detected by 12% SDS-PAGE (Fig. 3). Relatively high purity recombinant GST proteins were eluted by 100 mM imidazole and were dialyzed against sodium phosphate buffer (50 mM,

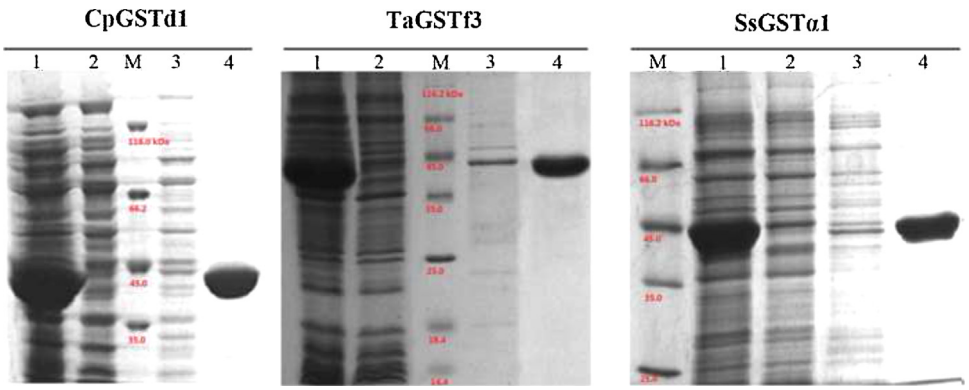

Fig. 3. Purification of recombinant GST proteins. *Lane* M: molecular mass marker proteins (MBI-Fermentas): β-galactosidase (116.0 kDa), bovine serum albumin (66.2 kDa), ovalbumin (45.0 kDa), lactate dehydrogenase (35.0 kDa) and REase Bsp98I (25.0 kDa); *Lane* 1: soluble fraction of recombinant GSTs; *Lane* 2: flow-through elution; *Lane* 3: wash-down elution; *Lane* 4: purified GSTs with 100 mM imidazole elution. The arrows indicate the expected size of purified recombinant GSTs.

pH 7.2) overnight at 4 °C. It can be seen that the soluble recombinant proteins all migrated as a single band after purification and their molecular mass was estimated to be approximately 45 kDa (reducing electrophoresis) due to an 18 kDa tag fusing at the N-terminal of the protein contributed by the pET-32a (+). After being subjected to a non-reducing electrophoresis, these GSTs were migrated as homodimers with a molecular mass of ~90 kDa, and the molecular mass of the subunit was ~45 kDa (27 kDa plus the 18 kDa tag).

3.5. Biochemical properties of GSTs

The CpGSTd1, SsGSTα1 and TaGSTf3 all showed their optimum activity under neutral or weak alkaline environment (Fig. 4). The

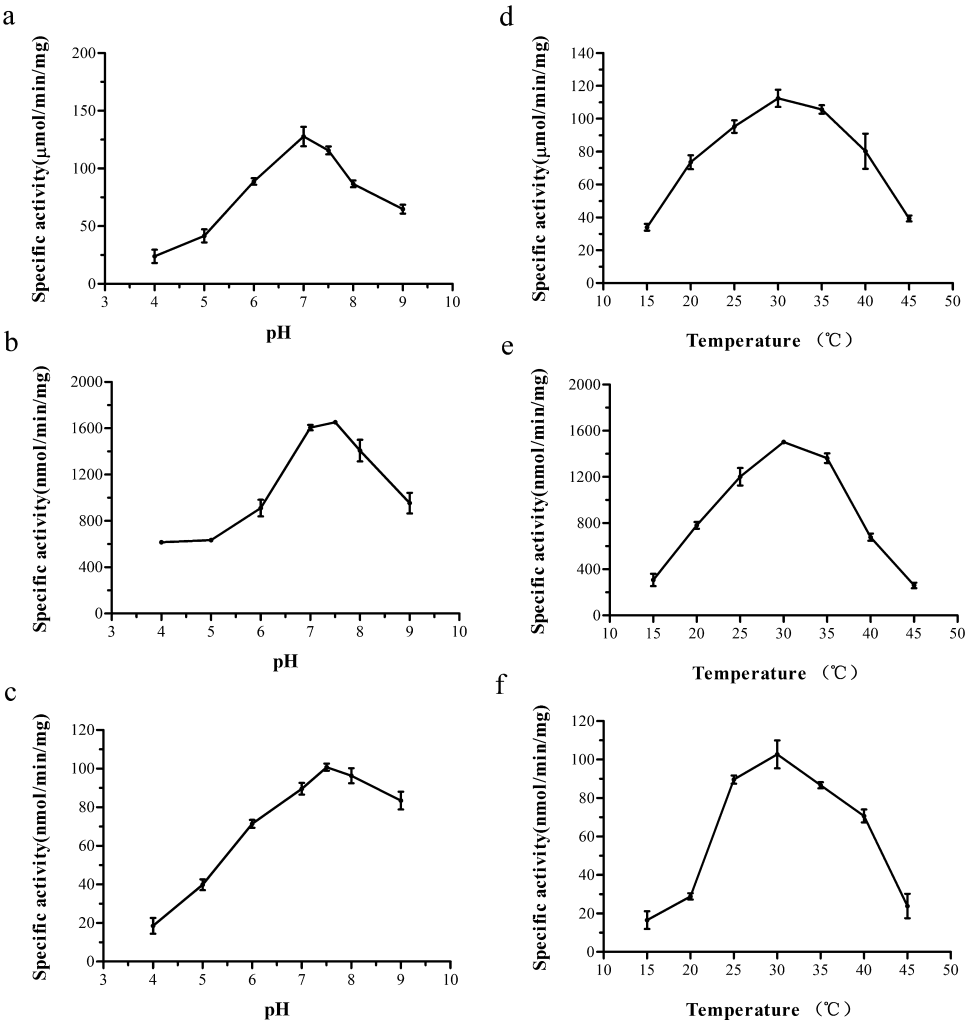

Fig. 4. Biochemical properties of GSTs. The effect of pH on the activity of CpGSTd1 (a), SsGSTα1 (b) and TaGSTf3 (c). The effect of temperature on the activity of CpGSTd1 (d), SsGSTα1 (e) and TaGSTf3 (f). The error bars represent the standard deviation (SD) of the mean of three replicates.

Table 2
Enzymatic kinetic parameters of the GSTs.

Proteins	CDNB				GSH			
	K_m (mM)	V_{max} (μmol/mg/min)	k_{cat} (min)	k_{cat}/K_m (mM/min)	K_m (mM)	V_{max} (μmol/mg/min)	k_{cat} (min)	k_{cat}/K_m (mM/min)
CpGSTd1[a]	0.27	121.7	3.66×10^4	1.37×10^5				
SsGSTα1	0.091	1.68	5.94×10^3	6.55×10^3	0.79	2.40	8.50×10^3	1.07×10^4
TaGSTf3	0.20	0.19	6.56×10^2	3.31×10^3	0.36	0.29	9.85×10^2	2.72×10^3

[a] The kinetic parameters have been reported in a previous study [11].

CpGSTd1 exhibited its maximum activity at pH 7.0 but activity was significantly reduced at pH 5.0 (Fig. 4a). The SsGSTα1 showed the highest activity for CDNB at pH 7.0 and 7.5, with significant reductions in activity at pH 6.0 and 9.0 (Fig. 4b). The optimum activity of the TaGSTf3 was observed at pH 7.0–8.0, and shows less than 40% of its maximum activity below pH 5.0 (Fig. 4c).

The temperature optima of CpGSTd1, SsGSTα1 and TaGSTf3 were investigated at temperatures ranging from 15 to 45 °C (Fig. 4). These GSTs showed relative thermal stability at 25–35 °C and optimum activity was observed at 30 °C (Fig. 4d–f).

The double-reciprocal Lineweaver–Burk plots of SsGSTα1, CpGSTd1 and TaGSTf3 catalyzed reactions with 0.01–1.6 mM of CDNB or 0.0625–4 mM of GSH were performed; results are shown in Table 2. The result indicates that the observed V_{max} and K_m values of SsGSTα1 are 1.68 μmol/min/mg and 0.091 mM for CDNB, whereas the values are 2.40 μmol/min/mg and 0.79 mM for GSH (Table 2). The K_m value of the TaGSTf3 for CDNB was 0.20 mM and for GSH was 0.36 mM. The TaGSTf3 also exhibited a V_{max} value of 0.19 μmol/min/mg for CDNB, but the value was 0.29 μmol/min/mg toward GSH (Table 2). A previous study demonstrated that the CpGSTd1 exhibited a V_{max} value of 121.7 μmol/min/mg and a K_m value of 0.27 mM toward CDNB, and the enzyme's catalytic constant k_{cat} and catalytic efficiencies (k_{cat}/K_m) were 3.66×10^4 min^{-1} and 1.37×10^5 $min^{-1}mM^{-1}$, respectively [11]. The k_{cat} and k_{cat}/K_m values of SsGSTα1 are as follows: 5.94×10^3 min^{-1} and 6.55×10^3 mM/min for CDNB, and 8.50×10^3 min^{-1} and 1.07×10^4 mM/min for GSH, respectively. For TaGSTf3, the k_{cat} and k_{cat}/K_m values were 6.56×10^2 min^{-1} and 3.31×10^3 mM/min for CDNB, and 9.85×10^2 min^{-1} and 2.72×10^3 mM/min for GSH, respectively. As shown in Table 2, CpGSTd1 possesses a higher affinity toward CDNB than SsGSTα1 and TaGSTf3.

3.6. Effects of cantharidin and its analogs on CpGSTd1 activities

In this study, cantharidin and its analogs were selected to investigate their effect on CpGSTd1 activity *in vitro*. The CpGSTd1 was significantly inhibited by pre-incubation of 4 mM cantharidin and cantharidic acid for 5 min, with approximately 2.85% and 14.53% of activity remaining, respectively (Fig. 5). The CpGSTd1 was slightly inhibited by 0.4 mM norcantharidin and norcantharidic acid, demethylated analog of cantharidin and cantharidic acid, respectively, with only 18.27 and 21.5% of activity impaired (Fig. 5).

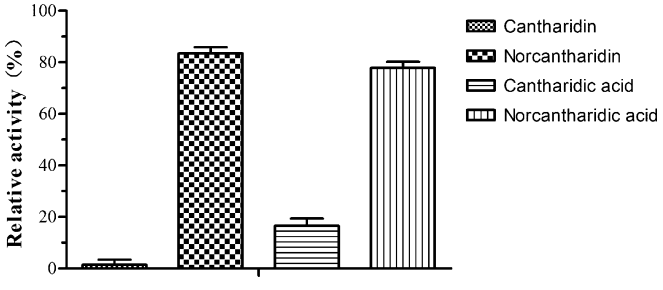

Fig. 5. Effects of cantharidin and its analogs on CpGSTd1 activities. CpGSTd1 was pre-incubated with final concentrations of 4 mM cantharidin, norcantharidin, cantharidic acid and norcantharidic acid at 30 °C for 5 min, respectively, before the addition of CDNB. The remaining activity was measured and the activity of CpGSTd1 protein without pre-incubated with cantharidin or its analogs was considered to be 100%. The error bars represent the standard deviation (SD) of the mean of three replicates.

3.7. Effects of cantharidin on GSTs activities

In this experiment, varying concentrations (0.02, 0.2, 2 mM) of cantharidin were used to measure their ability to inhibit the CpGSTd1, SsGSTα1, and TaGSTf3 on GSH–CDNB conjugation activity. The CpGSTd1 activity was 11.41 and 28.34% inhibited by 5 min pre-incubation with 0.02 and 0.2 mM cantharidin, respectively (Fig. 6a). The CpGSTd1 was strongly inhibited by 2 mM cantharidin, with 52.16% of activity remaining, suggesting that cantharidin shows an approximately IC_{50} value of 2 mM on CpGSTd1 activity. There was no significant difference in SsGSTα1 activity across all cantharidin concentrations used (Fig. 6a). Interestingly, the activity of TaGSTf3 was significantly activated by cantharidin, depending on

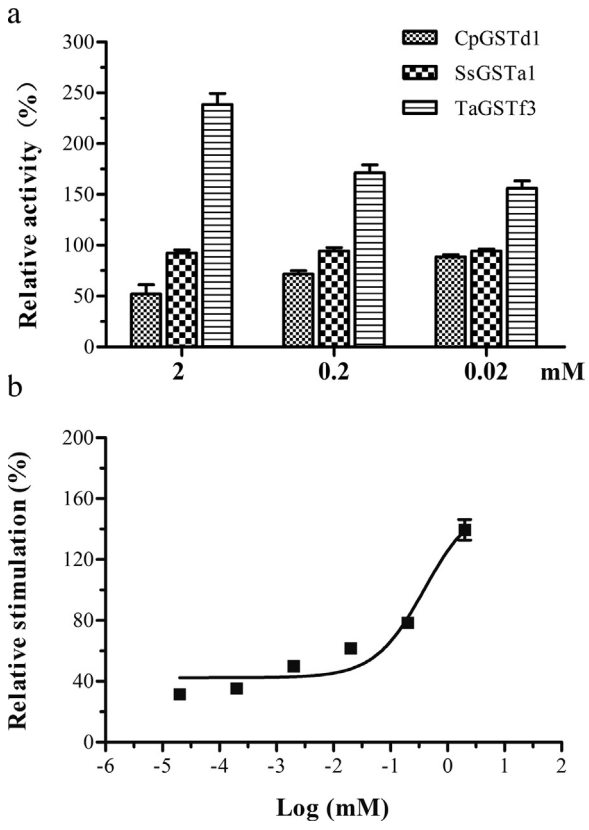

Fig. 6. Effects of varying cantharidin concentrations on CpGSTd1, SsGSTα1 and TaGSTf3 activities (a) and log (dose)-response stimulation of cantharidin on TaGSTf3 (b). Proteins were pre-incubated with different concentrations of cantharidin at 30 °C for 5 min before the addition of CDNB. The remaining activities were measured and the activities of CpGSTd1, SsGSTα1 and TaGSTf3 proteins without pre-incubated with cantharidin was considered to be 100%. The error bars represent the standard deviation (SD) of the mean of three replicates.

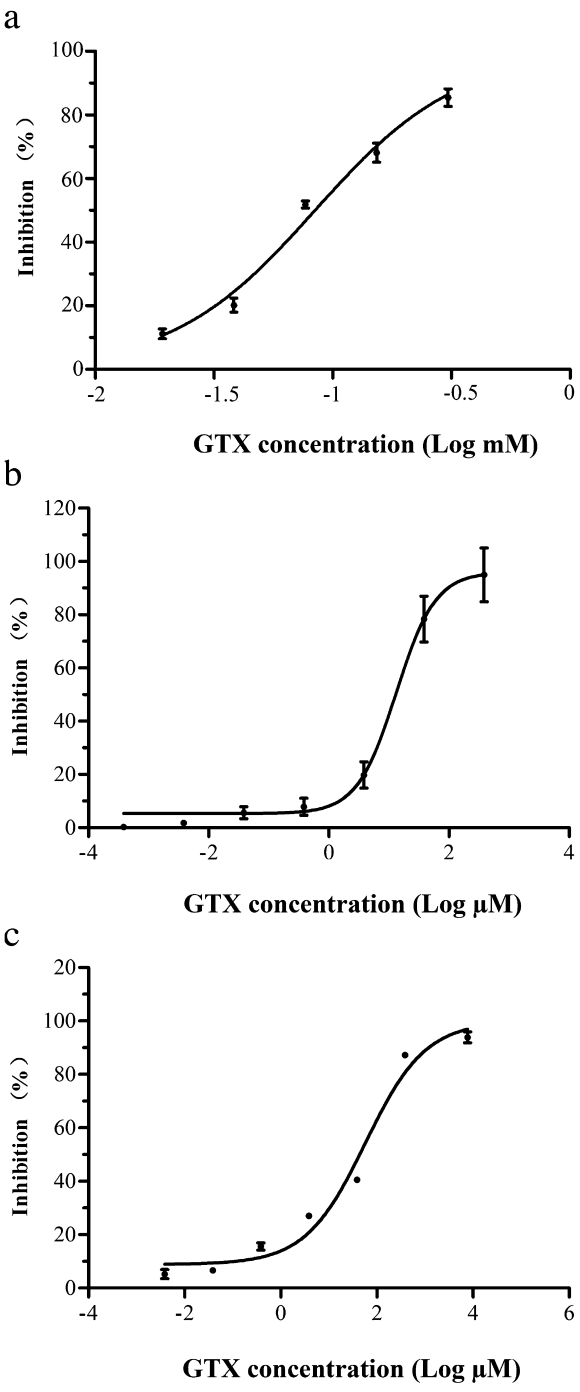

Fig. 7. IC_{50} plots of CpGSTd1 (a), SsGSTα1 (b) and TaGSTf3 (c) inhibition of CDNB conjugating activity by GTX.

the cantharidin concentration used (Fig. 6a). The observed TaGSTf3 activities were 1.56-, 1.71-, and 2.39-fold activated at 0.02, 0.2 and 2 mM of cantharidin, respectively (Fig. 6a). Log (dose)-response stimulation revealed that an approximately EC_{50} value of cantharidin on TaGSTf3 was 0.3852 mM (Fig. 6b). To further explain the results exhibited above, GTX, the competitive GST inhibitor was used to perform the positive control reactions on CpGSTd1, SsGSTα1 and TaGSTf3 (Fig. 7). Results revealed that GTX shows IC_{50} values of 84.28 [11], 13.22 and 57.68 μM for CpGSTd1, SsGSTα1 and TaGSTf3, respectively.

4. Discussion

GSTs are a superfamily of dimeric proteins responsible for catalyzing the conjugation of glutathione (GSH) with a wide range of endogenous and exogenous agents, including carcinogens, therapeutic drugs, insecticides, environmental toxins and products of oxidative stress [8–10]. In insects, there is great interest in GSTs due to their role in the metabolism of insecticides [23]. Previous study indicated that CpGSTd1 plays a key role in the metabolism of lambda-cyhalothrin and is potentially involved in the development of insecticide resistance in *C. pomonella*, and also demonstrated that the metabolism of insecticides is probably not its major function [11]. To explore the potential role of GST genes in response to cantharidin, we investigated the biochemical properties of recombinant GST proteins from three sources, including *S. scrofa*, *C. pomonella* and *T. aestivum*, and characterized their sensitivity to inhibitors and response to cantharidin and its analogs.

The predicted Mw of these GSTs are in line with the molecular mass of a cytosolic GST subunit ranging from 21 to 29 kDa [24]. A previous study [11] demonstrated that CpGSTd1 is composed of an N-terminal domain (residues 1–81) and a C-terminal domain (residues 91–215). Most cytosolic GSTs are composed of an N-terminal domain and a C-terminal domain, and the G-site is located at the N-terminal domain [25]. Moreover, the N-terminal domain of a cytosolic GST always contains a serine residue involved in catalysis [8]. The Val 53, Arg 67, Ala 68 and Ile 69 in CpGSTd1 that form the G-site are highly conserved in CpGSTd1, SsGSTα1 and TaGSTf3, suggesting that these residues are crucial for glutathione binding. It has been reported that Val 53 in CpGSTd1 is an important substrate binding-related residue since it contributes to the hydrogen bond formation with the substrate [11].

In the constructed phylogenetic tree, many GSTs are involved in detoxification of xenobiotics, including herbicides, parasiticides and insecticides. For instance, the phi and tau class GSTs from *Oryza sativa* GST [26], GST from *Ovis aries* [27] and epsilon class GST from *Aedes aegypti* [28] are xenobiotics detoxifying-related GSTs. Thus, phylogenetic relationship of CpGSTd1, SsGSTα1 and TaGSTf3 with the representative sequences from previously described GSTs indicates that CpGSTd1, SsGSTα1 and TaGSTf3 may play important physiological roles in response to exposure to cantharidin and its analogs.

Previous studies revealed that the mammal alpha class GST [10], insect delta class GST [29], and plant phi class GST [14] were homodimers or heterodimers with a molecular mass of 50–60 kDa. Most GSTs are active as dimers, composed of either homogeneous or heterogeneous subunits [14]. Thus, whether the CpGSTd1, SsGSTα1 and TaGSTf3 are dimers were further determined by non-reducing SDS-PAGE without β-mercaptoethanol or dithiothreitol added in the loading buffer (data not shown). Results suggested that the CpGSTd1, SsGSTα1 and TaGSTf3 were homodimers. The nucleophilic sulfhydryl group of glutathione, responsible for the conjugation reaction (also toward CDNB), is weakly acidic. Thus, the effects of pH on GST activities were performed at pH among 4.0–9.0. Results suggested that the maximum activity of CpGSTd1, SsGSTα1 and TaGSTf3 were determined in neutral and slight alkali environment. The optimal pH of CpGSTd1 is somewhat consistent with delta GST from *Culex pipiens* [30]. The optimal pH of SsGSTα1 and TaGSTf3 are in line with pi class GST from humans [31] and OsGSTU5 from *O. sativa* [26], respectively. The observed temperature optima of TaGSTf3 activity is not in line with OsGSTU5 from *O. sativa* [26]. It is known that the *Choristoneura fumiferana* GST, CfGST exhibits different biochemical properties when varying concentrations of glutathione or CDNB are used [29]. The V_{max} values of the SsGSTα1 for CDNB and GSH were much smaller than for alpha class GST from human colon adenocarcinoma cells, but the V_{max} of SsGSTf3 for both CDNB and GSH were all higher than alpha class

GST from human colon adenocarcinoma cells [32]. The K_m value of the TaGSTf3 for CDNB was 0.20 mM and for GSH was 0.36, which was in line with the published K_m value of OsGSTU5 from *O. sativa* [26]. A previous study demonstrated that the CpGSTd1 exhibited a V_{max} value of 121.7 μmol/min/mg and a K_m value of 0.27 mM [11].

A previous study demonstrated that cantharidin could potently block the activity of *Helicoverpa armigera* GST (HaGST) *in vivo* or *in vitro* [2]. The CpGSTd1 was significantly inhibited by 4 mM cantharidin and cantharidic acid, and was slightly inhibited by 4 mM norcantharidin and norcantharidic acid, demethylated analog of cantharidin and cantharidic acid, respectively, suggesting that the methyl group in cantharidin and cantharidic acid was favorable for binding to CpGSTd1 protein. This also could explain why the cantharidin possesses higher larvicidal activity than norcantharidin *Plutella xylostella* [16]. Removing the methyl group from cantharidin to form norcantharidin not only reduced the toxicity, but may also depress the protective response of an insect exposure to norcantharidin. The inactivation of CpGSTd1 activity by cantharidin probably is a reduced protective response. Although serine/threonine protein phosphatases are well known to be the target of cantharidin [5], GSTs are responsible for detoxification of xenobiotics, including carcinogens, therapeutic drugs, insecticides and herbicides, *etc.* [8–10]. We hypothesize that cantharidin likely has an inhibition or other effects on GSTs from other sources, such as mammals and plants.

A previous study suggests that cantharidin was an effective inhibitor of the total GSTs and the HaGST in the midgut of *H. armigera*, with a half-inhibitory concentration (IC_{50}) value of 9.77 and 12.5 μM, respectively [2]. To the best of our knowledge, the *Arabidopsis* [33] and *Oryza* [34] genomes contain 13 and 16 phi GSTs, respectively. They are mainly responsible for herbicide (endothall, *etc.*) detoxification together with class Tau GSTs [15]. In this study, the cantharidin shows an approximate IC_{50} value of 2 mM on CpGSTd1 activity, which is 160-fold higher than cantharidin on HaGST [2]. But, the activity of TaGSTf3 was significantly activated by cantharidin, with an approximate EC_{50} value of 0.3852 mM (Fig. 6b). The IC_{50} values of GTX on CpGSTd1, SsGSTα1 and TaGSTf3 suggest that the GST inhibitor GTX binds SsGSTα1 and TaGSTf3 more tightly than CpGSTd1. Increased enzyme activity of GST pre-incubated with cantharidin was in line with exposure of *T. aestivum* coleoptiles and roots to 3 mM Lead (Pb), which resulted in 150% and 280% of GST activity increase [35]. Increased GST activity was also observed after treatment of wheat shoots with 200 μM Ni [36]. Previous research demonstrated that GST plays an important role in the removal of toxic products of lipid and protein peroxidation [35] and GST may be involved in the resistance of plants to diverse environmental stresses [37].

Thus an unanswered question is raised: why are different results observed in varying GST sources by pre-incubation with cantharidin? It is well known that the GSTs play a key role in phase II of enzymatic detoxification [8]. GSTs have been found in both prokaryotic and eukaryotic organisms, including bacteria, yeasts, plants, insects and vertebrates [26]. They are involved in cellular detoxification and could detoxify carcinogens, therapeutic drugs, insecticides, herbicides, organic pollutants, and natural toxins, as well as the products of oxidative stress [8–10]. Cantharidin, a naturally occurring toxicant reported to possess insecticidal properties, has been developed into a bio-pesticide for pest control [2]. Its analog, endothall, a commercial herbicide, is widely used in the field [5]. It also possesses anti-cancer activity in mammals and has been used as a traditional Chinese medicine [38]. Phi and tau GST classes are the most studied GST groups involved in herbicide metabolism in maize [39]. Plant GSTs are responsible for detoxification of xenobiotics, as well as protecting cells from a wide range of biotic and abiotic stressors, including pathogen attack, heavy metal toxins, oxidative stress, and UV radiation [14]. Previous study has documented that plant GSTs were induced by herbicide safeners [40], herbicides [41,42] and chemicals [43], suggesting that these GSTs were involved in the protective responses. In this study, the CDNB-conjugating activity of TaGSTf3 was not inhibited but was activated by cantharidin, suggesting that the TaGSTf3 was involved in the protective responses to cantharidin exposure.

Cantharidin and its analog have been shown to inhibit mammalian [44] and plant [5] protein phosphatase activity, and the protein phosphatase family was thus confirmed to be the active target of these compounds [5]. In insects, cantharidin and its analog norcantharidin inhibit protein phosphatase activity [45]. In this study, the CpGSTd1 activity was significantly inhibited by cantharidin and cantharidic acid, suggesting that this GST protein binds well with cantharidin and cantharidic acid. It potentially participates in the detoxification process for cantharidin and cantharidic acid. It has been demonstrated that GSTs might facilitate the binding of insecticides with other enzymes, or act as binding proteins in a similar way to higher vertebrates providing passive protection [46]. In coding moth, the CpGSTd1 has been shown to probably associate with other more crucial functions aside from the metabolism of insecticides [11]. We hypothesize that the insect GSTs might act as binding proteins with cantharidin and its analogs before these xenobiotic compounds act on their target – phosphatases, which appears to be an insect defense mechanism in adapting to the threat posed by cantharidin and its analogs.

In summary, we report identification of glutathione *S*-transferase from three sources: SsGSTα1 from mammals, CpGSTd1 from insects and TaGSTf3 from plants, and characterize the molecular, phylogenetic, structural, biochemical and enzymological properties of their *E. coli*-produced recombinant proteins. Cantharidin and cantharidic acid show a strong inhibition effect on CpGSTd1 activity, whereas cantharidin has no effect on SsGSTα1 but significantly increases the activity of TaGSTf3, suggesting that this insect delta class GST, CpGSTd1, might act as a binding protein with cantharidin and its analogs. It also suggests that TaGSTf3 may be involved in the metabolism of cantharidin. Future work is required to perform molecular docking simulations, molecular dynamics (MD) and binding free energy calculation to structurally and energy-based answer why different results are observed in varying GST sources treatment with cantharidin, and how the GSTs are interacting with cantharidin. These findings might help us understand the mode of action of cantharidin and its analogs in living organisms.

Acknowledgements

We are grateful to Hao Feng and Haijin Liu (Northwest A & F University) for supplying the *S. scrofa* liver and *T. aestivum* lamina cDNAs, respectively. We also thank John Richard Schrock from Emporia State University (Emporia, KS, USA) for proofreading this manuscript before submission. This study is supported by the special fund for agro-scientific research in the public interest of China (No. 200903042 and 200903052).

References

[1] Ames BN, Profet M, Gold LS. Nature's chemicals and synthetic chemicals: comparative toxicology. Proc Natl Acad Sci U S A 1990;87:7782–6.
[2] Khan RA, Liu JY, Rashid M, Wang D, Zhang YL. Cantharidin impedes activity of glutathione *S*-transferase in the midgut of *Helicoverpa armigera* Hübner. Int J Mol Sci 2013;14:5482–500.
[3] Zhang YL, Zhou Y, Zhang ZY. Effect of cantharidin on the midgut of oriental armyworm (*Mythimna separata*) and diamond moth *Plutella xylostella*. Acta Entomol Sin 2003;46:272–6.
[4] Ma Y, Liu RR, Ma ZQ, Zhang YL. Effects of cantharidin on four metabolizing enzymes and PPO in *Mythimna separata* (Walker) (Lepidoptera Noctuidae). Acta Entomol Sin 2010;53:870–5.

[5] Li YM, Casida JE. Cantharidin-binding protein: identification as protein phosphatase 2A. Proc Natl Acad Sci U S A 1992;89:11867–70.
[6] Bajsa J, Pan Z, Dayan FE, Owens DK, Duke SO. Validation of serine/threonine protein phosphatase as the herbicide target site of endothall. Pestic Biochem Physiol 2012;102:38–44.
[7] Hayes JD, Pulford DJ. The glutathione *S*-transferase supergene family: regulation of GST and the contributions of the isoenzymes to cancer hemoprotection and drug resistance. Crit Rev Biochem Mol Biol 1995;30:445–600.
[8] Sheehan D, Meade G, Foley VM, Dowd CA. Structure, function and evolution of glutathione transferases: implications for classification of non-mammalian members. Biochem J 2001;360:1–16.
[9] Enayati AA, Ranson H, Hemingway J. Insect glutathione transferases and insecticide resistance. Insect Mol Biol 2005;14:3–8.
[10] Dourado DFAR, Fernandes PA, Ramos MJ. Mammalian cytosolic glutathione transferases. Curr Protein Pept Sci 2008;9:325–37.
[11] Liu JY, Yang XQ, Zhang YL. Characterization of lambda-cyhalothrin metabolizing glutathione *S*-transferase CpGSTd1 from *Cydia pomonella* (L.). Appl Microbiol Biotechnol 2014;98:8947–62.
[12] Ding YC, Ortelli F, Rossiter LC, Hemingway J, Ranson H. The *Anopheles gambiae* glutathione transferase supergene family: annotation, phylogeny and expression profiles. BMC Genomics 2003;4:35.
[13] Low WY, Feil SC, Ng HL, Gorman MA, Morton CJ, Pyke J, et al. Recognition and detoxification of the insecticide DDT by *Drosophila melanogaster* glutathione *S*-transferase D1. J Mol Biol 2010;399:358–66.
[14] Lan T, Yang ZL, Yang X, Liu YJ, Wang XR, Zeng QY. Extensive functional diversification of the *Populus* glutathione *S*-transferase supergene family. Plant Cell 2009;21:3749–66.
[15] Frova C. Glutathione transferases in the genomics era: new insights and perspectives. Biomol Eng 2006;23:149–69.
[16] Sun WB, Liu ZY, Zhang YL. Cantharidin and its anhydride-modified derivatives: relation of structure to insecticidal activity. Int J Mol Sci 2013;14:1–16.
[17] Reinemer P, Dirr HW, Ladenetein R, Huber P. Three-dimensional structure of class π glutathione *S*-transferase from human placenta in complex with *S*-hexylglutathione at 2.8 Å resolution. J Mol Biol 1992;227:214–26.
[18] Gasteiger E, Gattiker A, Hoogland C, Ivanyi I, Appel RD, Bairoch A. ExPASy: the proteomics server for in-depth protein knowledge and analysis. Nucleic Acids Res 2003;31:3784–8.
[19] McGuffin LJ, Bryson K, Jones DT. The PSIPRED protein structure prediction server. Bioinformatics 2000;16:404–5.
[20] Tamura K, Dudley J, Nei M, Kumar S. MEGA4: molecular evolutionary genetics analysis (MEGA) software version 4.0. Mol Biol Evol 2007;24:1596–9.
[21] Yang XQ, Zhang YL. Effect of temperature and sorbitol in improving the solubility of carboxylesterases protein *CpCE-1* from *Cydia pomonella* and biochemical characterization. Appl Microbiol Biotechnol 2013;97:10423–33.
[22] Bradford MM. A rapid and sensitive method for the quantification of microgram quantities of protein utilizing the principle of protein–dye binding. Anal Biochem 1976;72:248–54.
[23] Chen L, Hall PR, Zhou XE, Ranson H, Hemingway J, Meehan EJ. Structure of an insect δ-class glutathione S-transferase from a DDT-resistant strain of the malaria vector *Anopheles gambiae*. Acta Crystallogr D 2003;59:2211–7.
[24] Mannervik B, Danielson UH. Glutathione transferases-structure and catalytic activity. Crit Rev Biochem Mol Biol 1988;23:283–337.
[25] Yan H, Meng F, Jia H, Guo X, Xu B. The identification and oxidative stress response of a zeta class glutathione *S*-transferase (GSTZ1) gene from *Apis cerana* cerana. J Insect Physiol 2012;58:782–91.
[26] Cho HY, Yoo SY, Kong KH. Cloning of a rice tau class GST isozyme and characterization of its substrate specificity. Pestic Biochem Physiol 2006;86:110–5.
[27] Bártíková H, Køíová V, Štìpnièková M, Lamka J, Kubíèek V, Skálová L, et al. Activities of biotransformation enzymes and flubendazole metabolism in lambs (*Ovis aries*): effect of gender and flubendazole therapy. Pharmacol Rep 2010;62:362–73.
[28] Lumjuan N, Rajatileka S, Changsom D, Wicheer J, Leelapat P, Prapanthadara L, et al. The role of the *Aedes aegypti* epsilon glutathione transferases in conferring resistance to DDT and pyrethroid insecticides. Insect Biochem Mol Biol 2011;41:203–9.
[29] Feng QL, Davey KG, Pang ASD, Primavera M, Ladd TR, Zheng SC, et al. Glutathione *S*-transferase from the spruce budworm, *Choristoneura fumiferana*: identification, characterization, localization, cDNA cloning, and expression. Insect Biochem Mol Biol 1999;29:779–93.
[30] Samra AI, Kamita SG, Yao HW, Cornel AJ, Hammock BD. Cloning and characterization of two glutathione *S*-transferases from pyrethroid-resistant *Culex pipiens*. Pest Manag Sci 2011;68:764–72.
[31] Kolm RH, Sroga GE, Mannervik B. Participation of the phenolic hydroxyl group of Tyr-8 in the catalytic mechanism of human glutathione transferase P 1-1. Biochem J 1992;285:537–40.
[32] Zhang K, Wong KP, Chow P. Conjugation of chlorambucil with GSH by GST purified from human colon adenocarcinoma cells and its inhibition by plant polyphenols. Life Sci 2003;72:2629–40.
[33] Dixon DP, Lapthorn A, Edwards R. Plant glutathione transferases. Genome Biol 2002;3:1–10.
[34] Soranzo N, Gorla MS, Mizzi L, Toma GD, Frova C. Organisation and structural evolution of the rice glutathione *S*-transferase gene family. Mol Genet Genomics 2004;271:511–21.
[35] Lamhamdi M, Bakrim A, Aarab A, Lafont E, Sayah F. Lead phytotoxicity on wheat (*Triticum aestivum* L.) seed germination and seedings growth. C R Biol 2011;334:118–26.
[36] Gajewska E, Sklodowska M, Slaba M, Mazur J. Effect of nickel on antioxidative enzyme activities, proline and chlorophyll contents in wheat shoots. Biologia Plant 2006;50:653–9.
[37] Davis DG, Swanson HR. Activity of stress-related enzymes in the perennial weed leafy spurge (*Euphorbia esula* L.). Environ Exp Bot 2001;46:95–108.
[38] Mebs D, Pogoda W, Schneider M, Kauert G. Cantharidin and demethylcantharidin (palasonin) content of blister beetles (Coleoptera: Meloidae) from southern Africa. Toxicon 2009;53:466–8.
[39] Cummins I, O'Hagan D, Jablonkai I, Cole DJ, Hehn A, Werck-Reichhart D, et al. Cloning, characterization and regulation of a family of phi class glutathione transferases from wheat. Plant Mol Biol 2003;52:591–603.
[40] Taylor VL, Cummins I, Brazier-Hicks M, Edwards R. Protective responses induced by herbicide safeners in wheat. Environ Exp Bot 2013;88:93–9.
[41] Moons A. Regulatory and functional interactions of plant growth regulators and plant glutathione *S*-transferases (GSTs). Vitam Horm 2005;72:155–51202202.
[42] Dixon DP, Skipsey M, Edwards R. Roles for glutathione transferases in plant secondary metabolism. Phytochemistry 2010;71:338–50.
[43] Malik JA, Goel S, Kaur N, Sharma S, Singh I, Nayyar H. Selenium antagonises the toxic effects of arsenic on mungbean (*Phaseolus aureus* Roxb.) plants by restricting its uptake and enhancing the antioxidative and detoxification mechanisms. Environ Exp Bot 2012;77:242–8.
[44] Li YM, Mackintosh C, Casida JE. Protein phosphatase 2A and its [^{3}H]cantharidin/[^{3}H]endothall thioanhydride binding site: inhibitor specificity of cantharidin and ATP analogues. Biochem Pharmacol 1993;46:1435–43.
[45] Chen X, Liu JY, Zhang YL. Cantharidin impedes activity of protein serine/threonine phosphatase in *Plutella xylostella*. Mol BioSyst 2014;10:240–50.
[46] Kostaropoulos I, Papadopoulos AI, Metaxakis A, Boukouvala E, Papadopoulou-Mourkidou E. Glutathione *S*-transferase in the defence against pyrethroids in insects. Insect Biochem Mol Biol 2001;31:313–9.